

# Fiber Network Model for Reduced Order Composite Multi-Scale Models

Scott E Stapleton, 1 Sagar Shah2

University of Massachusetts Lowell, Lowell, MA, 01854, U.S.A.

By taking advantage of repeating geometry found in fiber reinforced microstructures, a reduced order model was created where the only degrees of freedom exist at fiber centerlines, making for an efficient model compared to traditional continuum finite element models. The formulation of the model is briefly discussed, and some initial comparisons are made for linear elastic fields and strength predictions with finer, higher-fidelity models.

#### I. Introduction

Miromechanical models have been created for fiber reinforced composite materials in order to predict the homogenized composite properties based on fiber and matrix constitutive properties[1]. This has been shown to be very useful in many different applications, with finite element (FE) models being the most common microscale models. These models are primarily 2-D, which allows the models to be more efficient and even able to be coupled concurrently with larger-scale finite element models.

However, these micromodels have a few potential limitations. First, recent research has shown that the fibers are not all parallel and aligned, but entanglement exists between fibers [2–5]. It is unclear how this entanglement effects homogenized composite properties, but it has been speculated that transvers fracture and failure inition may be sensitive to fiber entanglement [2]. To ascertain this effect computationally, a representative volume element (RVE) large enough to represent the entanglement must be modelled, which may push the feasability limits of traditional FE models [6]. Second, dense mesh requirements due to high gradients a between near-touching or touching fibers can prohibit model size. Alternatively, many chose to enforce a minimum distance between fibers to eliminate the need for a dense mesh, but this changes the microstructure and altres sites likely to instigate failure.

To overcome these to potential limitations, a reduced order model has been created for fiber-scale RVEs. The model was based on the discrete element method (DEM), and the only degrees of freedom are the fiber centerline displacements and rotations. The model assumes that the majority of the load transfer occurs between fiber neighbors. A linear displacement field is assumed between fibers, and the effect of the matrix on fibers is found by integrating the stresses at the fiber/matrix interface. In this way, the matrix can be reduced to springs connecting fibers, while still being able to extract stress fields for application of failure theories. Progressive damage is captured by removing material between the fibers and changing the bounds of integration for the forces. The model will be presented along with comparisons with traditional FE models to judge the relative accuracy.

#### II. Method

# A. Formulation

Looking at the stress distribution in the matrix of a transversely loaded composite microstructure shown in Figure 1, the load appears to be running from the top to the bottom in load branches (red is for high stress). These load branches are constructed of repeated elements: two fibers with matrix in between them with the critical region being the thinnest part of the matrix between the two fibers. The stresses in the matrix-rich regions are often much

1

American Institute of Aeronautics and Astronautics

<sup>&</sup>lt;sup>1</sup> Associate Professor, Mechanical Engineering, University Ave. 1, Lowell, MA 01854, Senior AIAA Member.

<sup>&</sup>lt;sup>2</sup> Research Assistant, Mechanical Engineering, University Ave. 1, Lowell, MA 01854, non-AIAA Member.

lower (blue and green), making these regions less critical in predicting stress fields. This shows that the critical regions of the matrix within the microstructure is made of repeating, connected geometries. Therefore, for densely packed fibers, one could create a model where care is taken to represent stress fields in the matrix between close fiber neighbors as the primary means of load transfer, and other mechanisms such as stress in matrix pockets or stress between fiber pairs further apart can be approximated with less fidelity. For the Fiber Network Model, the load transfer between fibers through the matrix is reduced to springs connecting fiber centers, creating a network of springs connecting fibers as shown in Figure 1. Through this reduction, a micro-model could be made with 4 degrees of freedom per fiber, rather than 10's or 100's in continuum FE models, enabling fast models that can be used to generate relatively large training data sets needed for machine learning.

The Fiber Network Model is built on a Discrete Element Method (DEM) framework. Each fiber is modeled as a line-mass, and Newton's equations of translational and rotational motion are solved using a predictor-corrector scheme and 5th order Gear's integration method. Fiber neighbors are identified through Delaunay triangulation, and the cost-savings of the model lies in deriving the "equivalent spring" forces of the matrix between each fiber neighbor pair. A corotational reference frame is used as the local pair-wise coordinate system and local displacements are assumed to vary linearly between the fibers (local y-direction). Once the displacement field is fully defined between the fibers as shown in Figure 2, stress and strain can be derived. For the base model, small strains and linear elastic materials are used to allow a closed-form expression for the forces. Therefore, this base model is linear elastic with large rotations and small strains. Nonlinear strain and stress expressions can be utilized, though a closed-form solution becomes less likely. While this model seems to only consider matrix between fiber pairs, the fact that the top and bottom surfaces of the matrix between fiber pairs doesn't end in a traction-free boundary gives stresses at the edges similar to global stress levels found in resin-rich regions. Finally, the force that the matrix exerts on each fiber is found by integrating the surface traction at the fiber/matrix interface. This integral can be found close-formed for linear elastic materials and small strains, which eliminates discretization.

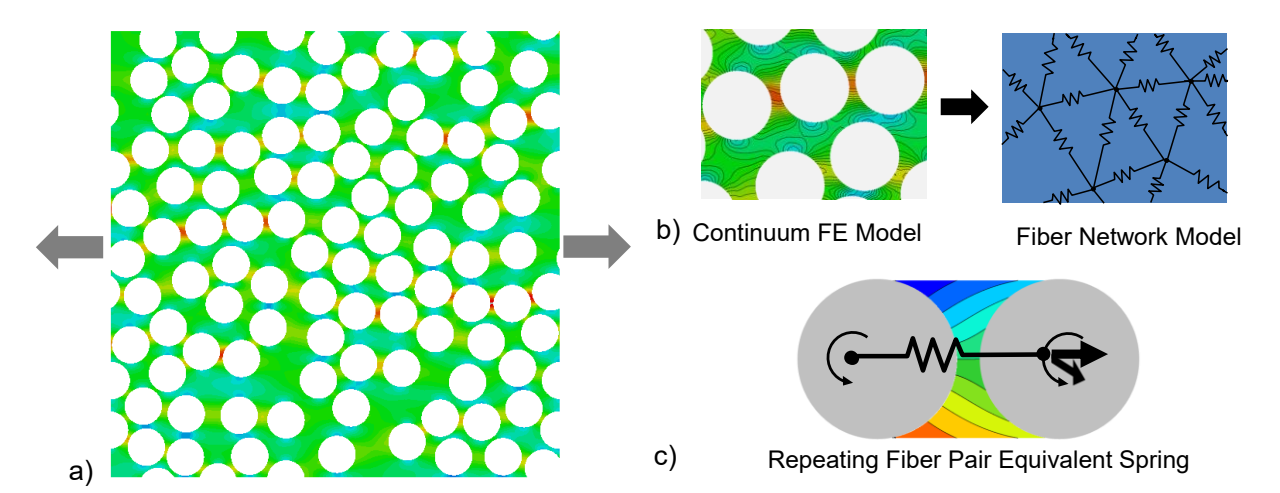


Figure 1. The stress distribution a) of a transversely loaded composite microstructure shows the highest stresses in the matrix connecting fiber pairs in load branches from the left to the right of the model. b) The repeating elements of two fibers with matrix between were simplified to reduce the order of the model. By isolating a fiber pair and solving for the equivalent force as a function of fiber centerline displacements, a fiber-reinforced continuum model can be approximated by a series of springs between fiber centerpoints.

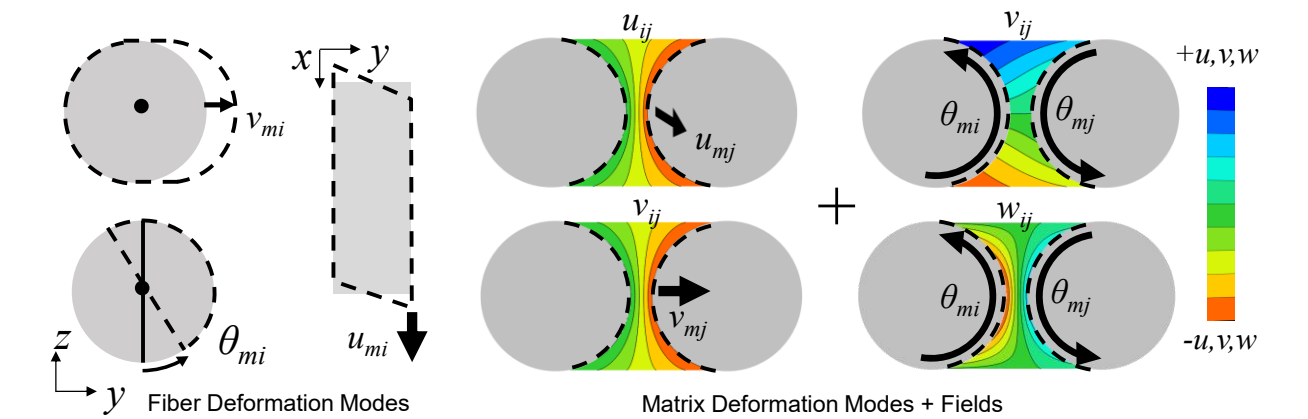


Figure 2. Fiber deformation modes are approximated using simple closed-form solutions, and matrix displacement fields are found by linear interpolation between neighboring fibers.

Finally, when the stress between two fibers reaches a critical value defined by some failure criteria, that portion of matrix is eliminated by simply changing the boundaries of integration between the fibers. In this way, smeared cracks can develop progressively through the model with a fraction of the computational needs of a continuum model with equivalent capabilities.

While there are certainly many aspects of the local fields which are not correctly represented, it is a hope that these aspects play only minor roles in the strength and stiffness predictions.

## B. Model Comparison with 2-D Continuum Model

The Fiber Network Model (FNM) was compared with a 2-D finite element (FE) continuum model to determine whether the model successfully captured the behavior of an RVE under transverse loading. This 2-D continuum FE model was created using the Abaqus/Explicit commercial software package. An RVE size of 50 fibers was chosen based on the microstructure convergence study performed by Shah et al. [7]. Ten periodic RVEs were generated comprised of a random dispersion of IM7 carbon fiber (fiber diameter of 6 µm) in the RIM R135/H1366 epoxy matrix. The ten microstructure renditions were produced at a volume fraction of 0.55 with the aid of a random RVE generator developed by Stapleton et al. [8,9]. Perfect bonding was assumed between the fiber and matrix. The fibers were modeled as transversely isotropic solids, the thermo-mechanical properties of which are summarized in Table 1, and the matrix properties are shown in Table 2. Each RVE was meshed with C3D8R (eight-node, brick elements with reduced integration). An average mesh size of 0.075 x the fiber diameter was chosen.

A dynamic explicit analysis was carried out in Abaqus/EXPLICIT to test the RVEs under transverse tension. The RVEs were subjected to mechanical loading by prescribed a velocity boundary condition. Flat boundary conditions were enforced during this analysis. Failure in the RVEs was modeled with a progressive damage model [7] based on the crack band theory [10], implemented within Abaqus/EXPLICIT with the VUMAT user-written subroutine. The maximum principal stress criterion was used to define failure initiation. A traction-separation law, governed by the fracture energy, defined the post-peak softening behavior.

Table 1. Constituent mechanical properties of IM7 carbon fiber.

$ ho^{ m f}$	1780	[kg/m3]
		[8
$E_{\mathrm{fl}1}$	276,000	[MPa]
$E_{\rm f33}$	19,500	
$\nu_{\rm f13}$	0.28	[-]
	0.25	
	$= \nu_{\rm f23}$	$v = v_{f23}$ 0.25

Shear Modulus	$G_{\rm fl2} = G_{\rm fl3}$	70,000	[MD-1
	$G_{f23}$	7,800	[MPa]

Table 2. Constituent thermo-mechanical properties of RIM R135/H1366 epoxy matrix.

Property		Value	Unit
Density	$ ho_{ m m}$	1200	[kg/m <sup>3</sup> ]
Elastic Modulus	$E_{\mathrm{m}}$	2482	[MPa]
Poisson's ratio	$\nu_{ m m}$	0.37	[-]
Critical Strength	$\sigma_{mcr}$	64.1	[MPa]
Fracture Toughness	$G_{\text{mIC}}$	0.001	$[J/m^2]$

For the FNM model, the same material properties were used. However, rather than a progressive failure scheme, material was deleted when it reached the maximum principal stress equal to the critical strength. Periodic boundary conditions were imposed by projecting edge fibers to the other side of the RVE, and the projected fiber shared forces and displacements with the original fiber as explained in [8]. Equilibrium was solved using a Newton-Raphson scheme with the loading of broken up into 100 load steps and allowing 10 iterations per load step. Upon equilibrium, the matrix was checked for failure, and failed material was removed. After removal, the load step was re-applied until equilibrium was found, and the process was repeated. This was repeated a maximum of 20 times until the crack reached growth equilibrium. The stiffness matrix for the system was calculated at the beginning of the load step, and then only updated upon failure. Additionally, a characteristic distance of 0.005 x the radius of the fiber to keep the solution away from singularities at the extreme of the fibers. The homogenized stress vs strain results were compared between the two models, along with the stiffness and strength.

#### C. Effect of Fiber Distribution on Strength and RVE Size Convergence

Finally, a small example study was run to demonstrate the usefulness of the model in running large amounts of simulations in very little time. For the example, RVEs from 36 to 900 fibers were created, with 100 repetitions of each RVE size. The RVE generation techniques developed in [9] were used to make RVEs with three different degrees of fiber aggregation. The RVEs were generated by randomly seeding the fibers, then running a simulation with penalty contact enforced until the kinetic energy of the system subsides. The contact damping of the fibers,  $d_c$ , was varied at  $d_c = 0.1$ , 0.25, and 0.5, where a value of 1.0 indicates critical damping. Increasing the contact damping increases the propensity of fibers to stick together or aggregate, while less damping causes fibers to spread out more homogenously. To properly study these effects, a model needs to be able to run a large amount of repetitions and fairly large volumes, which makes is exactly what the FNM model was designed for.

#### III. Results

## A. Model Comparison with 2-D Continuum Model

Initial validation of the model was done by comparing the Fiber Network Model (FNM) with a dense-mesh continuum finite element model of a hexagonally packed microstructure and transverse loading as shown in Figure 3. The displacement fields predicted between two fibers is illustrated in the contour. The main displacement, v, showed only 5% deviation between the two models, probably owing to the simplification of fiber deformation in the FNM. However, the transverse displacement, w, is not considered in the FNM though it shows up in the continuum model, albeit at a much lower magnitude. This means that the main tensile stresses between fibers are accurately represented, deviations can come from incorrect multi-axial strain state representation in the FNM model. The degree to which this plays a role will depend on the failure theory applied to the matrix.

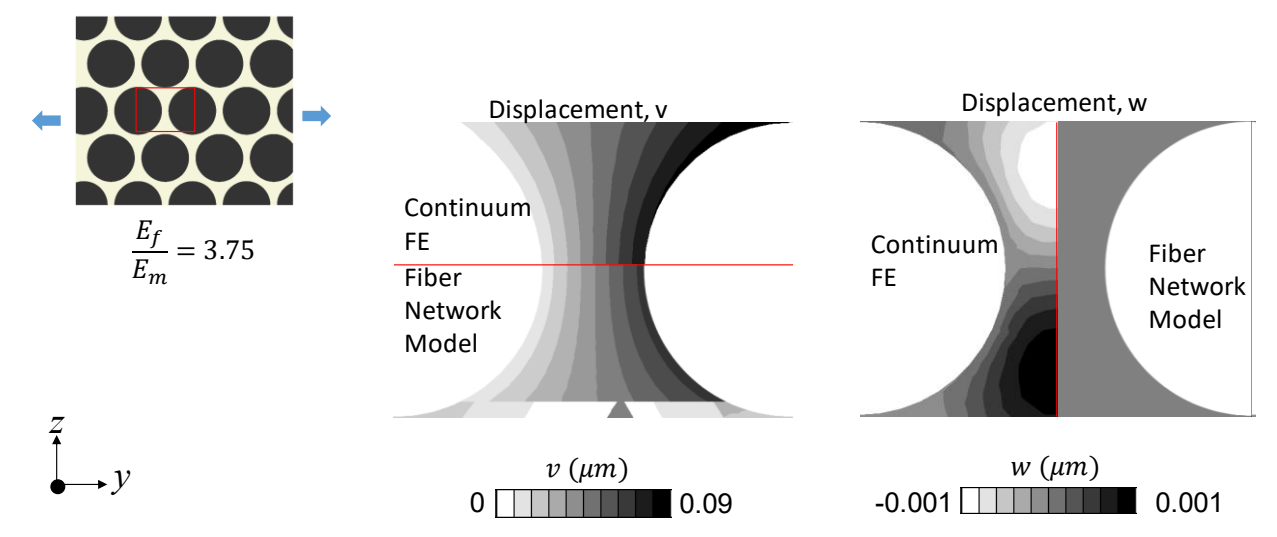


Figure 3. Comparing stress fields between the Fiber Network Model (FNM) and continuum finite element model for a hexagonally packed microstructure showed that the displacement field in the direction between the fiber centerpoints was represented within 5%, but the FNM was over constrained transversely.

The FNM model was also compared with a finite element continuum model with continuum damage and element deletion. While both the continuum model and FNM are still being tuned and improved upon, initial results are shown here. Figure 4 shows a comparison between the homogenized stress/strain response for one of the repetitions. The FNM model was consistently stiff, and it was hypothesized that the restriction of transverse deformation caused the matrix to be overly constrained and a "restrained modulus" effect. To relieve this constraint, the Poisson's ratio of the matrix was set to 0 so that any axial displacement would not induce transverse strains. This alteration caused the stiffness of the two models to agree much more closely, and a poison's ratio of 0 was utilized for the rest of the study.

Another blatant difference between the two models was the post-peak behavior. The Continuum model showed brittle failure, while the FNM failure was much more progressive. It is believed that stress localization that occurs in continuum models does not occur in the FNM, since the displacement field is restricted to being linear. In other studies, not shown here, close fiber pairs were more accurately predicted while more distant fiber neighbors seemed to be too strong. It is hypothesized that the larger distance is not captured as well with a linear strain field, and the fracture energy release is not necessarily preserved. Further iterations of the model will include an energy-preserving failure formulation.

Figure 5 shows a comparison of the strength and stiffness of all samples between the continuum, FNM, and FNM with Poisson's ratio set to 0. Setting the poison's ratio to 0 improved both the stiffness and strength prediction in nearly every case, showing that the constrained modulus effect did indeed play a meaningful role. In general, the model appeared to predict the stiffness within 10% and strength within 15%.

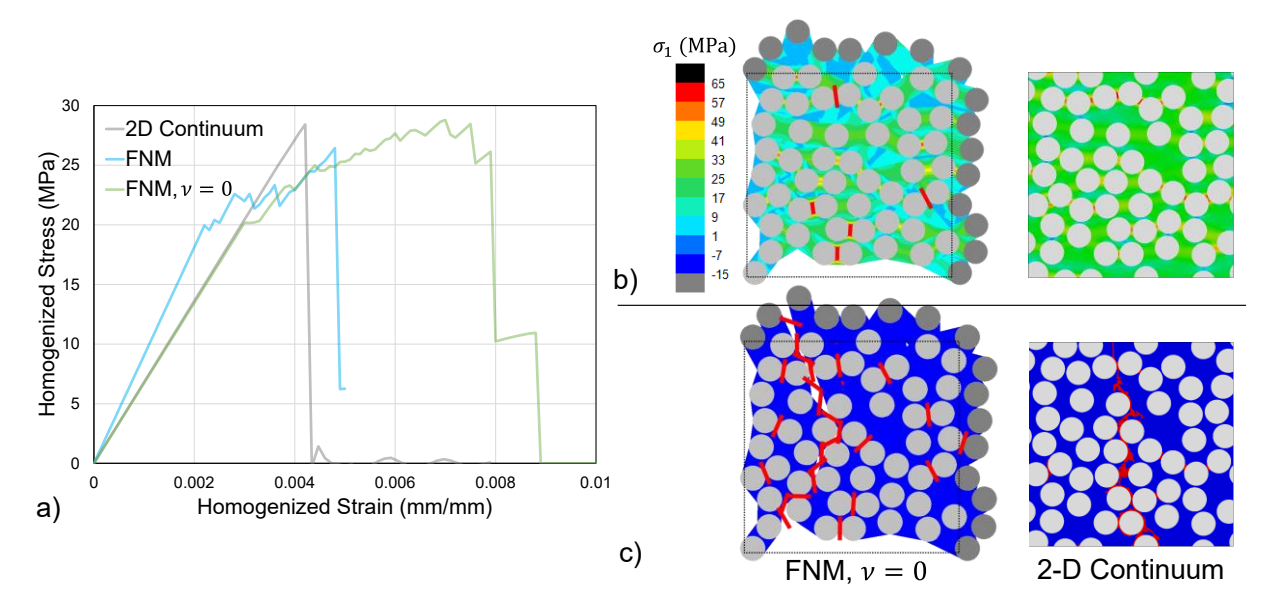


Figure 4. Comparison of one repetition of the Fiber Network Model and the 2-D Continuum FE model, showing the a) response, b) stresses at a strain of 0.0042, and b) final state showing the crack path in red.

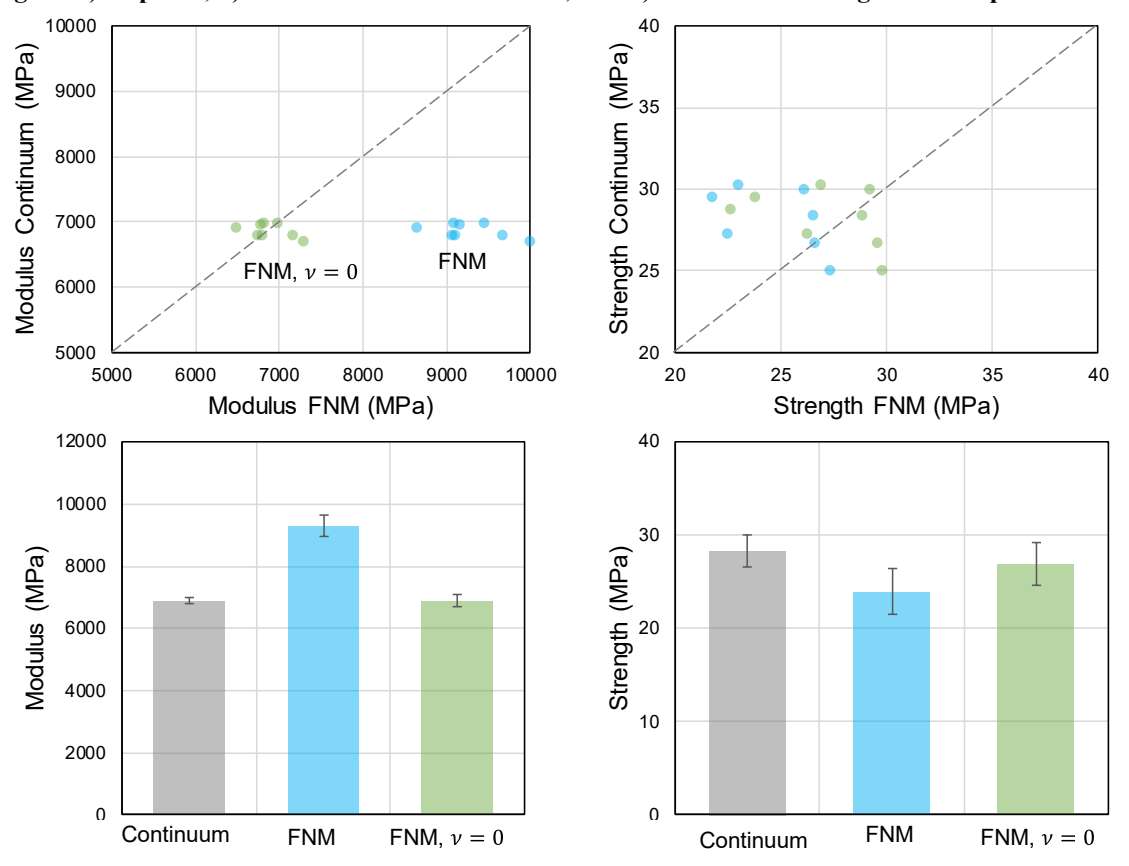


Figure 5. Results comparing the modulus and strength of the fiber network model (FNM) against a traditional, dense-mesh finite element continuum model. FNM simulations ran in the order of minutes, while Continuum FE models ran for 1-7 days.

#### B. Effect of Fiber Distribution on Strength and RVE Size Convergence

Finally, a small example study was run to demonstrate the usefulness of the model. Figure 6 shows an RVE convergence study for microstructures with different amounts of fiber aggregation. Two RVEs with 900 fibers each are shown for each value of  $d_c$  on the right, while the average of 100 repetitions at each RVE size for each value of  $d_c$  are shown on the right. Looking at the randomly selected RVEs, one can observe that the  $d_c$ =0.1 RVEs are much more homogenously spaced, while increasing the damping results in more aggregation of fibers. These aggregations result in higher stress concentrations between fibers, and large matrix spaces tend to cause greater load to travel through the fibers around the space. Therefore, the strength of the RVEs with more aggregation failed earlier in general, with the average decrease between specimens reaching around 10%.

A second thing to note from the plot in Figure 6 is how the average strength values behave with increasing RVE size. The more fibers there are in the RVE (larger the RVE size), the earlier the RVE fails. This is probably due to the probability of "flaws", which has been reported by researchers in different fields [11,12]. The basic idea is that the larger the volume over which the maximum stress is applied, the more likely that there is a critical flaw in the volume that will fail prematurely. Therefore, the strength asymptotes at a large volume, but changes quite a bit for smaller volumes. This is distinctly illustrated in this study, where the size effect can be easily observed. One thing to note is that the more homogenous RVEs,  $d_c$ =0.1, appeared to converge to a strength value for the volumes tested, while the other two did not. This supports the idea of critical flaws changing the strength, because more homogenous RVEs are going to have less critical flaws and when there are flaws, they will not be large enough to bring the strength down much. Many smaller RVEs that are seen in literature have less variation in fiber spacing and therefore, show very little size effect. This homogenous spacing may be more prevalent in very high-volume fraction composites where significant variation is not afforded due to the dense packing of fibers, but for mid-range composites the clustering can be as significant as those shown here.

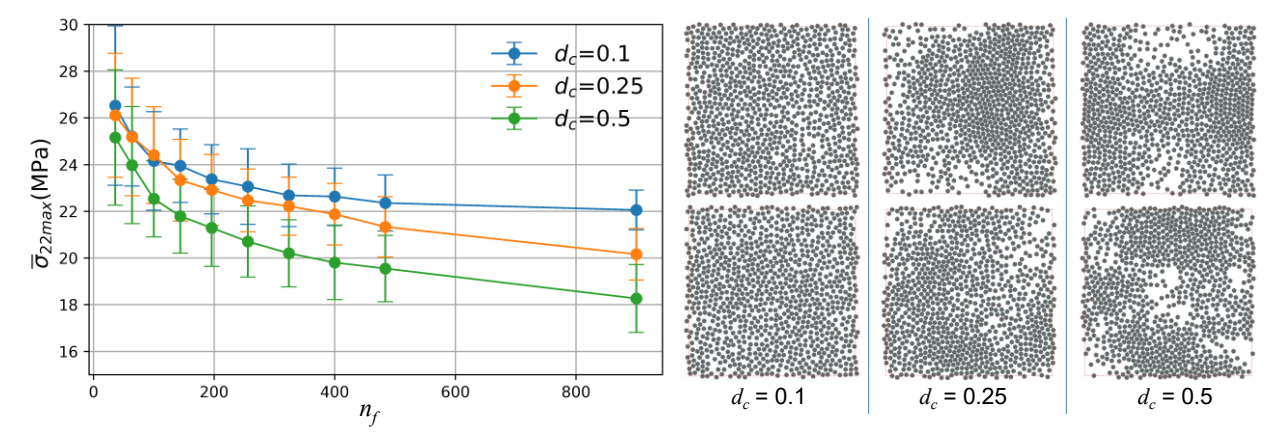


Figure 6. Preliminary results of using the model to generate large amounts of data. The contact damping during packing generation,  $d_c$ , controls the fibers propensity to aggregate. This study shows the RVE size convergence by plotting strength vs number of fibers in the RVE,  $n_f$ .

## IV. Conclusions

In this study, a Fiber Network Model (FNM) was created to capture the main mechanism involved in stress concentrations and failure initiation of fiber reinforced composite microstructures loaded in the transverse direction, and thereby make an ultra-efficient micro-model for use in multi-scale and stochastic studies. The main mechanism identified was the load transfer between nearest neighbor fibers. The deformation field between two fibers was simplified and used to create equivalent springs to represent the matrix. A comparison was made between the FNM and a more traditional 2-D Continuum FE model, and the FNM was shown to predict the stiffness within 10% and strength within 15%. While fidelity is decreased for the FNM model, the computational time is drastically improved. The FNM model ran on a normal PC in under a minute, while the Continuum model took 1-7 days on a

high-performance machine. Therefore, for applications where speed is vital like multi-scale modelling, the loss of fidelity may be well worth the speedup.

Finally, a small parametric study was conducted to demonstrate the usefulness of the model. The number of fibers in an RVE was varied between 36 and 900, and the RVE generation parameters were changed to produce different levels of fiber clustering. From the study, it appears that more clustered fibers may lead to a slightly lower strength, though variation between samples is rather significant. Additionally, a size effect observed experimentally in brittle and semi-brittle materials was observed, though more homogenously spaced fiber RVEs showed less of a size effect due to a decreased prevalence of failure-prone fiber arrangements. Such a study with this many repetitions and this size of fibers would not be feasible for many current models, showing a case for such a lower fidelity model. In any case, though significant improvements could still be made to the FNM, this demonstrates the concept of utilizing ultra-efficient models to enable data-driven studies of the variability of microstructures of composite materials.

# V. Acknowledgements

This material is based upon work supported by the NASA Transformational Tools and Technologies (TTT) program under grant 80NSSC21M0102 and work supported by the National Science Foundation and Air Force Office of Scientific Research under Grant No. 1826232. Any opinions, findings, and conclusions or recommendations expressed in this material are those of the authors and do not necessarily reflect the views of the National Science Foundation.

#### VI. References

- [1] Aboudi, J., Arnold, S. M., and Bednarcyk, B. A. Micromechanics of Composite Materials: A Generalized Multiscale Analysis Approach. Butterworth-Heinemann, 2012.
- [2] Fast, T., Scott, A. E., Bale, H. A., and Cox, B. N. "Topological and Euclidean Metrics Reveal Spatially Nonuniform Structure in the Entanglement of Stochastic Fiber Bundles." *Journal of Materials Science*, Vol. 50, No. 6, 2015, pp. 2370–2398. https://doi.org/10.1007/s10853-014-8766-2.
- [3] Czabaj, M. W., Riccio, M. L., and Whitacre, W. W. "Numerical Reconstruction of Graphite/Epoxy Composite Microstructure Based on Sub-Micron Resolution X-Ray Computed Tomography." *Composites Science and Technology*, Vol. 105, 2014, pp. 174–182. https://doi.org/10.1016/j.compscitech.2014.10.017.
- [4] Sanei, S. H. R., Barsotti, E. J., Leonhardt, D., and Fertig, R. S. "Characterization, Synthetic Generation, and Statistical Equivalence of Composite Microstructures." *Journal of Composite Materials*, Vol. 51, No. 13, 2017, pp. 1817–1829. https://doi.org/10.1177/0021998316662133.
- [5] Stapleton, S., Schey, M., Przybyla, C., Uchic, M., Krieger, H., Appel, L., and Zabler, S. Comparison of Fiber Microstructural Characteristics for Two Grades of Carbon Fiber Composites. In *American Society for Composites — Thirty-third Technical Conference*, No. 0, Seatle, WA, 2018.
- [6] Mathew Schey, Scott Stapleton, Przybyla, C., Uchic, M., and Zabler, S. Determining a Length Scale of FRP Composite Microstructures. In American Society for Composites — 34Technical Conference, No. 0, Atlanta, Georgie, 2019.
- [7] Shah, S. P., and Maiarù, M. "Effect of Manufacturing on the Transverse Response of Polymer Matrix Composites." *Polymers*, Vol. 13, No. 15, 2021, p. 2491. https://doi.org/10.3390/polym13152491.
- [8] Stapleton, S. E., Appel, L., Simon, J.-W., and Reese, S. "Representative Volume Element for Parallel Fiber Bundles: Model and Size Convergence." *Composites Part A: Applied Science and Manufacturing*, Vol. 87, 2016, pp. 170–185. https://doi.org/10.1016/j.compositesa.2016.04.018.
- [9] Stapleton, S. E., Husseini, J. F., Schey, M. J., Beke, T., and Pineda, E. J. Statistical Descriptors of Composite Fiber Aggregation. Presented at the 35th ASC Technical Conference, Jersey City, NJ, 2020.
- [10] Bažant, Z. P., and Oh, B. H. "Crack Band Theory for Fracture of Concrete." *Matériaux et Construction*, Vol. 16, No. 3, 1983, pp. 155–177. https://doi.org/10.1007/BF02486267.

- [11] Arndt, C. M., de Carvalho, N. V., and Czabaj, M. W. "Experimental Reexamination of Transverse Tensile Strength for IM7/8552 Tape-Laminate Composites." *Journal of Composite Materials*, Vol. 54, No. 23, 2020, pp. 3297–3312. https://doi.org/10.1177/0021998320914065.
- [12] Rypl, R., Chudoba, R., Mörschel, U., Stapleton, S. E., Gries, T., and Sommer, G. "A Novel Tensile Test Device for Effective Testing of High-Modulus Multi-Filament Yarns." *Journal of Industrial Textiles*, 2014, p. 1528083714521069. https://doi.org/10.1177/1528083714521069.